DOI 10.5162/IMCS2012/P1.8.8

Fabrication and properties of an OLED-based gas sensor with poly(3-hexylthiophene) sensing film

Guangzhong Xie, Yadong Jiang, Xiaosong Du, Huiling Tai, Weizhi Li
School of Optoelectronic Information, State Key Laboratory of Electronic Thin Films and Integrated Devices, University of Electronic Science and Technology of China, Chengdu, 610054, China
gzxie@uestc.edu.cn

Abstract

An OLED-based gas sensor is fabricated with the device structure as ITO/*N,N*'-bis(naphthalen-1-yl)-*N,N*'-bis(phenyl)-benzidine (NPB)(30 nm)/tris(8-hydroxy-quinolinatoo)aluminium (Alq_3)(50 nm)/poly(3-hexylthiophene-2,5-diyl) (P3HT)(x nm)/Mg: Ag (300 nm). The P3HT is applied as the sensitive layer in the OLED-based gas sensor, while red light emission can be observed from the OLED. The response of the device in NO_2 and NH_3 circumstance is investigated respectively by analyzing its effect on variation of the current density. The results show that the NO_2 concentration has an obvious influence on the current density of the device, and the current density decreases faster under the higher NO_2 concentration. Meanwhile, the current density of the device increases when it is exposed in the NH_3 circumstance. The sensing mechanism of the device is also discussed.

Key words: Sensor, OLED, P3HT, NO_2, NH_3

Introduction

The gas sensor is related to high technology on chemical science, material science and so on. Its production is simple and inexpensive, so it has been widely applied to industrial production control, family life safety, food industry, medical test, environmental protection and etc. The gas sensor with different sensing films can detect inflammable, explosive and toxic gases.

The gas sensor is moving toward small sizes, being integrated and multi-functional. OLED has recently become one of the most promising techniques for future display and lighting applications because of high brightness, wide viewing angle, low-cost, low power, wide working temperature range and many other advantages[1]. So far OLED is used in displays and starting for lighting applications. The organic materials are excited by the electric field to give out the light. It is a light-emitting process from electric energy to light energy.

OLED-excited, PL-based sensors present a promising approach for developing compact, low-cost, sensitive, selective, and fast-response sensor arrays for a variety of analytes and real-world applications [2-4]. A structurally integrated O_2 sensor, where the OLED pixel array and an oxygen sensor film are fabricated on glass substrates that are attached back-to-back, was successfully demonstrated; the resulting module was ~2 mm thick [3]. The sensing was based on O_2-induced quenching of the PL intensity and shortening of the PL decay time of the oxygen-sensitive dyes Pt octaethylporphyrine (PtOEP) or the Pd analog PdOEP embedded in a thin polystyrene (PS) film, due to dye-O_2 collisions [5-8]. The OLED-based O_2 sensor served also as a basis for monitoring other analytes such as glucose, lactate, and ethanol by monitoring oxygen consumption during the oxidation reactions of the above-mentioned analytes in the presence of an appropriate specific oxidase enzyme [2,3].

Moreover, the design of flexible OLEDs, the wavelength tunability, and the pixel outline, together with the ability to individually address the pixels, enable utilization of the OLED platform for simultaneous detection of multiple analytes in mixtures [3]. In this platform, an array of OLED pixels, which is structurally integrated with the sensing elements, is used as the photoluminescence (PL) excitation source. The structural integration is achieved by fabricating the OLED array and the sensing element on opposite sides of a common glass substrate or on two glass substrates that are attached back-to-back. As it does not require optical fibers, lens, or mirrors, it results in a uniquely simple, low-cost, and potentially rugged geometry. Changes in the PL intensity I and decay time caused by the analytes are tested in this platform [9-11].

Experimental

In this paper, we described an OLED-based gas sensor with the device structure as: ITO/*N,N*'-bis(naphthalen-1-yl)-*N,N*'-bis(phenyl)-benzidine (NPB, 30 nm)/tris(8-hydroxy-quinolinatoo)aluminium (Alq_3, 50 nm)/poly(3-hexylthiophene-2,5-diyl) (P3HT, x nm)/Mg: Ag (300 nm), as shown in figure 1. ITO-coated substrate was ultrasonically cleaned with detergent, de-ionized water, acetone, and ethanol step by step, and then dried by nitrogen blow. It was treated by oxygen plasma for 5 *min* to increase the wok function. Organic layers (NPB and Alq_3) and metallic cathode were subsequently deposited at the rates of 0.1~0.3 *nm/s* and 1~2 *nm/s*, respectively, while keeping the pressure on the order of magnitude 10^{-4} and 10^{-3} *Pa* respectively, without breaking the vacuum. Film thickness and deposition rate were monitored *in situ* by oscillating quartz thickness monitors. On the other hand, the P3HT was spin coated at 800/2000 rpm and 1000/3000 rpm for devices A and device B, respectively, resulting in different thickness for P3HT. The current density and luminance of the devices in NO_2 environment was tested and analyzed in self-designed platform. Electroluminescent (EL) spectra of the devices were measured with an OPT-2000 spectrometer and the luminance-bias voltage-current density (*L-V-J*) characteristics were recorded with a Keithley 4200 source.

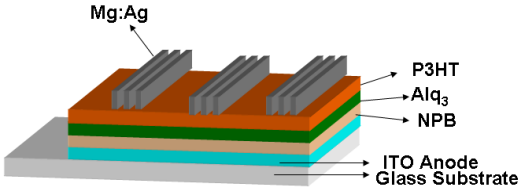

Fig. 1: The device structure of the OLED-based gas sensor.

Results and discussions

The electroluminescence property of the OLED-based gas sensor

Figure 2 shows the EL spectra of devices A and B. In device A, there is a peak at 664 nm and 648 nm at the bias voltage of 11 and 12 V respectively, while in device B, there is a peak at 650 nm at 11 V. In addition, a shoulder at 725 nm in the EL spectra is also observed in both devices A and B. Thus, it is known that the device shows red emission, ascribing to P3HT.

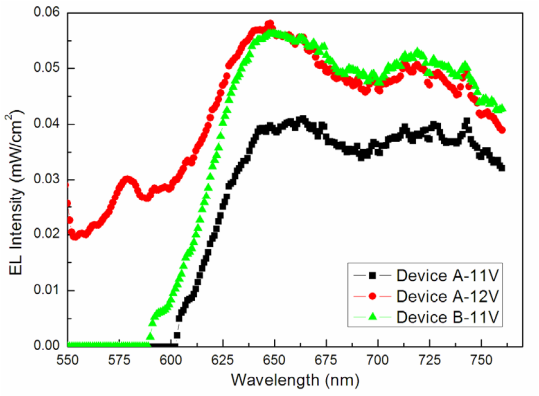

Fig. 2: The electroluminescent spectra for devices A and B.

The electrical property of OLED-based gas sensor

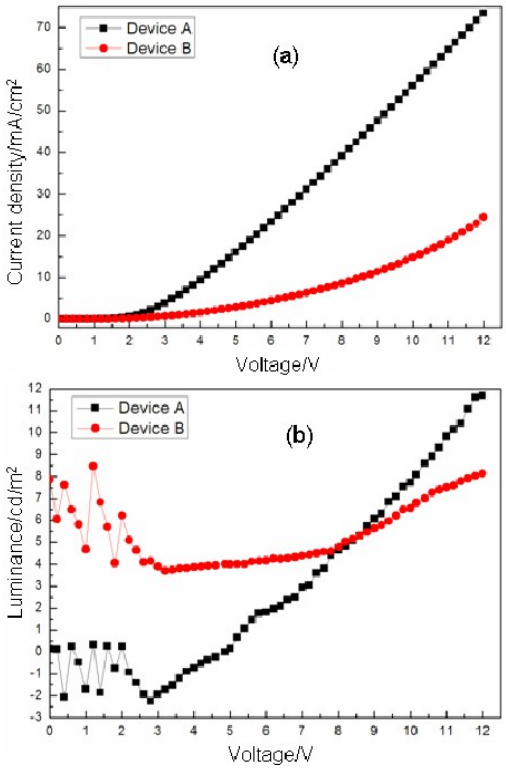

Fig. 3: (a) The J-V and (b) L-V characteristics of the OLED-based gas sensor.

Fig. 3(a) shows the J-V characteristics of devices A and B. As shown in Fig. 3(a), the current density of devices A and B is very small at the low voltage, which increases fast with the increasing voltage. On the other hand, the current density of device A is relatively larger than that of device B at the same voltage. Fig. 3(b) displays the luminance-voltage characteristics (L-V) of the devices. The L-V curves are in agreement with the J-V characteristics behavior. It can be seen that, at the low driving voltage, the luminance of device A is lower than that of device B. However, the luminance of device A is higher than the

luminance of device B when the voltage is higher than 8 V. The luminance of the devices is low mainly due to low efficiency of P3HT and spin-coating method, and the performance of the device can be further improved. The sensing property of the OLED-based sensor was measured using device A, considering that the luminance of device B is very low.

The sensing property of OLED-based sensor

1. In NO_2 circumstance

The current density of device A in 50 ppm NO_2 and N_2 circumstance is shown in Fig. 4, while the driving voltage of the device is 12 V, while the inset shows relative change of the current density. As can be seen that, the current density show similar behavior in both 50 ppm NO_2 and N_2 circumstance. At the first 10 min, the current density slight decreases, while the current density decreases more rapidly in 50 ppm NO_2 circumstance after then. After 90 min, the current density is reduced to be 99.3 % in the ppm N_2 circumstance, while the current density is reduced by 1.1 % in the ppm NO_2 circumstance, from 73.5 mA/m^2 to 72.6 mA/m^2. Consequently, it can be known that NO_2 has an effect on the device, by reducing the current density.

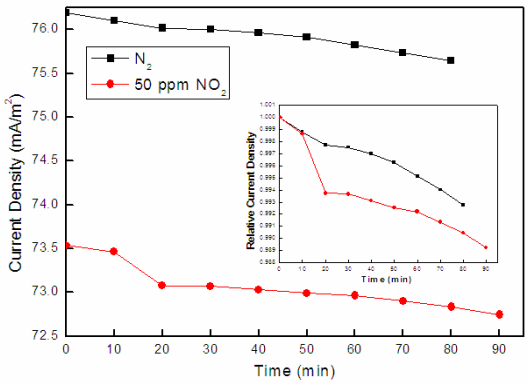

Fig. 4: Variation of the current density in device A at 50 ppm NO_2 and N_2 circumstance.

The current density of device A in 20 ppm, 50 ppm and 80 ppm NO_2 circumstance is shown in Fig. 5, while the driving voltage of the device is 12 V. The variation of the current density is normalized. It can be learned that, with the time increasing, the current density of the device decreases when it is exposed in the three different NO_2 concentrations. Moreover, under the NO_2 concentrations of 20 ppm, the current density shows a relatively small decrease with compared to that in 50 ppm and 80 ppm NO_2 circumstance. For example, the current density is reduced to be 0.991 mA/m^2 after 90 min under the NO_2 concentrations of 20 ppm, while it is 0.988 mA/m^2 in 80 ppm NO_2 circumstance. The results indicate that the oxidative gas NO_2 has a great influence on device performance.

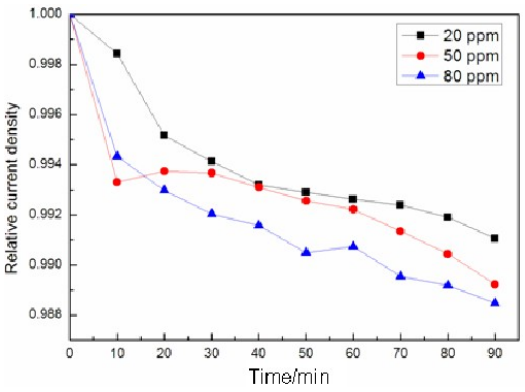

Fig. 5: Variation of the current density in device A at NO_2 circumstance.

2. In NH_3 and N_2 circumstance

The current density of device A in 250 ppm NH_3 and N_2 circumstance is shown in Fig. 6, the inset shows the relative change of the current density, while the operating voltage of the device is 12 V. The variation of the current density is normalized. It is obviously shown that, as the time increases, the current density slightly decreases when it is exposed in the N_2 circumstance. On the other hand, when it is exposed in 250 ppm NH_3 circumstance, the current density gradually increases from 87.5 mA/m^2 to 91 mA/m^2, showing an enhancement of 4%. The results indicate that the device is very sensitive to the reductive gas NH_3, while the inert N_2 can be utilized for protective gas.

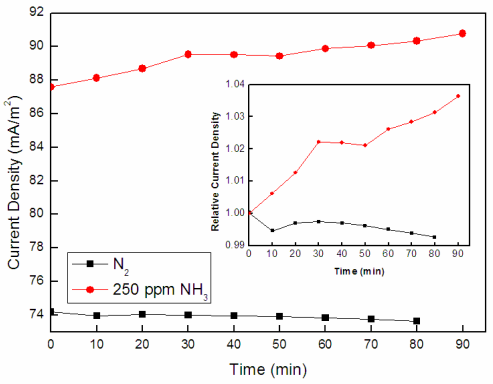

Fig. 6: Variation of the current density in device A at 250 ppm NH_3 and N_2 circumstance.

It is reported that, when the gas is adsorbed by n-type or p-type semiconductor, a space-charge region is generated on its surface, forming the surface energy. Therefore, the surface energy or Fermi energy of the semiconductor is changed, resulting in electron donating and accepting relation between the gas and the semiconductor. As is known that, P3HT is P-type semiconductor. There will be a space-charge

region on its surface after adsorbing the oxidative gas, such as NO_2, leading to the increased contact barrier between P3HT and the metal cathode and reduced current density. On the contrary, the contact barrier will be reduced if the reductive gas, such as NH3 is adsorbed, thereby enhancing the current density. The mechanism for the NO_2 adsorption process by P3HT is given as Fig. 7.

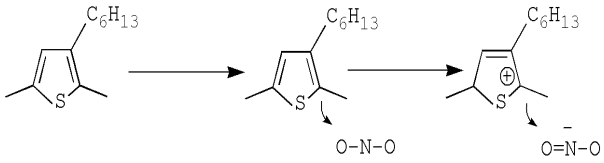

Fig. 7: The NO_2 adsorption process by P3HT.

In conclusion

An OLED-based gas sensor is fabricated, using the P3HT as sensitive layer, while red light emission can be observed from the OLED. Studies about the effect of NO_2, NH_3 and N2 on the current density of the device are demonstrated. The results show that the current density will decrease with exposure in the oxidative NO_2, and the current density decreases faster under the higher NO_2 concentration. However, the current density will increase with exposure in the reductive NH_3. These can be explained by the space-charge region caused by adsorption of the gas. If the gas is oxidative, the contact barrier between P3HT and metal cathode is increased, leading to reduced current density. As for the reductive gas, the contact barrier will be reduced to enhance the current density.

Acknowledgements

This work was partially supported by National Science Foundation of China (NSFC) through Grant No. 61176066 and by the Program for New Century Excellent Talents in University (Grant No. NCET-08-0088).

References

[1] Birnstock Jan, Hofmann Michael, Murano Sven, Vehse Martin, Blochwitz-Nimoth Jan; Huang Qiang, He Gufeng, Pfeiffer Martin, Leo Karl, Late-news paper: Novel OLEDs for full color displays with highest power efficiencies and long lifetime, SID Symposium Digest of Technical Papers 36, 40-43 (2005);doi: 10.1889/1.2036459

[2] B. Choudhury, R. Shinar, J. Shinar, Glucose biosensors based on organic light-emitting devices structurally integrated with a luminescent sensing element, Journal of Applied Physics 96, 2949-2954 (2004); doi: 10.1063/1.1778477

[3] R. Shinar, C. Qian, Y. Cai, Z. Zhou, B. Choudhury, J. Shinar, Structurally integrated organic light-emitting device (OLED)-based multianalyte sensing through analyte-oxidase interactions, Processing of SPIE 6007, 600710-1 (2005); doi: 10.1117/12.629699

[4] R. Shinar, Z. Zhou, B. Choudhury, J. Shinar, Structurally integrated organic light emitting device-based sensors for gas phase and dissolved oxygen, Analytica Chimica Acta 568, 190-199 (2006); doi: 10.1016/j.aca.2006.01.050

[5] O. S. Wolfbeis, L. Weis, M. J. P. Leiner, W. E. Ziegler, Analytical Chemistry 60, 2028-2030 (1988); doi: 10.1021/ac00170a009

[6] H. Weigl, A. Holobar, W. Trettnak, I. Klimant, H. Kraus, P. O'Leary, O. Wolfbeis, Journal of Biotechnology 32, 127-138 (1994); doi: 10.1016/0168-1656(94)90175-9

[7] Z. Rosenzweig, R. Kopelman, Sensors and Actuators B-Chemical 475, 35-36 (1996); doi: 10.1016/s0925-4005(97)80116-5

[8] Y. Amao, Michrochimica Acta 1, 1-12 (2003); doi: 10.1007/s00604-003-0037-x

[9] Rosenzweig Zeev, Kopelman Raoul Analytical properties of miniaturized oxygen and glucose fiber optic sensors, Sensors and Actuators, B: Chemical 36, 475-483(1996)

[10] LU X, MANNERS I, WINNIK M. A. Polymer/silica composite films as luminescent oxygen sensors. Macromol 34, 1917 -1927(2001); doi: 10.1021/ma001454j

[11] Roche P., Al-Jowder R., Narayanaswamy R., Young J., Scully P. A novel luminescent lifetime-based optrode for the detection of gaseous and dissolved oxygen utilising a mixed ormosil matrix containing ruthenium. Analytical and Bioanalytical Chemistry 386, 1245-1257(2006); doi: 10.1007/s00216-006-0787-5